

A first principles study on the electronic and magnetic properties of $\text{Ba}_{1-x}\text{K}_x\text{Fe}_2\text{As}_2$

Jun Dai,¹ Zhenyu Li,¹ Jinlong Yang,^{1,*} and J. G. Hou¹

¹*Hefei National Laboratory for Physical Sciences at Microscale,*

University of Science and Technology of China, Hefei, Anhui 230026, P.R. China

(Dated: August 1, 2008)

Abstract

We report a systematic first-principles study on the recent discovered superconducting $\text{Ba}_{1-x}\text{K}_x\text{Fe}_2\text{As}_2$ systems ($x = 0.00, 0.25, 0.50, 0.75$, and 1.00). Previous theoretical studies strongly overestimated the magnetic moment on Fe of the parent compound BaFe_2As_2 . Using a negative on-site energy U , we obtain a magnetic moment $0.83 \mu_B$ per Fe, which agrees well with the experimental value ($0.87 \mu_B$). K doping tends to increase the density of states at fermi level. The magnetic instability is enhanced with light doping, and is then weaken by increasing the doping level. The energetics for the different K doping sites are also discussed.

PACS numbers:

I. INTRODUCTION

The recent discovery of superconductivity in LaFeAs[O,F] has intrigued tremendous interest in layered FeAs systems.¹ Intensive studies have revealed that, by substituting La with Ce, Sm, Nd, Pr, and Gd,^{2,3,4,5,6} the superconducting temperature (T_c) can be raised from 26 up to 53.3 K, and even higher (about 55 K) under high pressure.^{7,8} As we know, the parent compound of the these superconductors has a tetrahedral ZrCuSiAs-type structure with alternate stacking of tetrahedral FeAs layers and tetrahedral LaO layers, and favors a stripe like antiferromagnetic (AFM) ground state. The parent compound is not a superconductor but a poor metal with high density of states and low carrier density.⁹ The ground state of the parent compound is supposed to be a spin density wave (SDW) ordered state with a stripe like AFM configuration.^{10,11} Superconducting occurs when the SDW instability is suppressed by replacing of O with F or importing O vacancies (electron doping), or Sr substituting of La (hole doping).^{2,12,13}

Very recently, the family of FeAs-based supercondutors has been extended to double layered RFe₂As₂ (R=Sr,Ba,Ca).^{14,15,16,17,18,19} The electronic structure of the parent compound has been studied both experimentally^{20,21,22} and theoretically.^{23,26,27} The density of states of RFe₂As₂ is very similar to that of ReFeAsO around the fermi level, so does the fermi surface. The magnetic order of BaFe₂As₂ has been revealed by experiment,²⁴ and the magnetic moment on Fe is $0.87 \mu_B$. Besides, SDW anomaly has also been found in the RFe₂As₂ systems.²⁰

Although the superconducting mechanism of these new superconductors is still unclear, the peculiar properties of the FeAs layers, especially the magnetic properties, are believed to be very important for understanding the origin of the superconductivity in these compounds. Although theoretical works have been reported for the double layered FeAs superconductors, the doping structure, magnetic coupling, as well as the the electronic structure after doping have not been thoroughly investigated. Besides, the magnetic moment on Fe atom obtained from previous theoretical studies is much larger than the experimental value (cal. $2.67 \mu_B$ v.s. exp. $0.87 \mu_B$).^{23,24} Similar problem has been encountered for the single layered ReFeAsO superconductors, and it was suggested that a negative on-site energy U should be applied to such systems.²⁸ It is interesting to see if such a remedy also works for BaFe₂As₂. Although the use of a negative U is counterintuitive, it is physically possible. As suggested

in a very recent work,²⁹ in itinerant systems, for d⁶ configuration as Fe²⁺ is, the exchange-correlation effect may cause charge disproportionation ($2d^6 \rightarrow d^5 + d^7$) and lead to $U = E(N+1) + E(N-1) - 2E(N) < 0$.

In this paper, we report the theoretical electronic and magnetic properties of Ba_{1-x}K_xFe₂As₂ ($x = 0.00, 0.25, 0.50, 0.75$, and 1.00) from first-principles calculations in the framework of generalized gradient approximation(GGA)+U. With a negative U , we obtain a magnetic moment per Fe atom for BaFe₂As₂ equal to 0.83 μ_B . By comparing the total energies, we predict the most favorable doping structure. Moreover, we find slight doping (x near or small than 0.25) tends to enhance the magnetic instability, while medium and heavy dopings (x near or larger than 0.5) tend to suppress it.

II. MODEL AND METHOD

BaFe₂As₂ exhibits the ThCr₂Si₂-type structure (space group *I4/mmm*), where FeAs layers are separated by single Ba layers along the c axis as shown in fig.1 (a). The FeAs layers are formed by edge-shared FeAs₄ tetrahedra, similar to that in ReFeAsO. In the calculation, we adopt a $\sqrt{2} \times \sqrt{2} \times 1$ supercell, which contains four Ba atoms, eight Fe atoms, and eight As atoms. All structures are fully optimized until force on each atom is smaller than 0.01 eV/Å. During all the optimizations and static calculations, the lattice parameters are fixed to the experimental values $a = b = 5.53$ Å and $c = 13.21$ Å.¹⁴ Although the lattice constants are different at different doping levels, the variations are very small, and we think they will not significantly change the electronic structures of the systems. To simulate doping, we replace one, two, three, and four Ba atoms with K atoms, which corresponds to 25%, 50%, 75%, and 100% doping, respectively.

The electronic structure calculations are carried out using the Vienna *ab initio* simulation package³⁰ within GGA+U.³² The electron-ion interactions are described in the framework of the projected augment waves method and the frozen core approximation.³¹ The energy cutoff is set to 400 eV. For density of states (DOS) calculation, we use a $12 \times 12 \times 6$ Monkhorst dense grid to sample the Brillouin zone, while for geometry optimization , a $6 \times 6 \times 3$ Monkhorst grid have been used. The on-site Coulomb repulsion is treated approximately within a rotationally invariant approach, so only an effective U, defined as $U_{eff}=U-J$ needs to be determined, where U is the on-site Coulomb repulsion (Hubbard U) and J is the atomic-

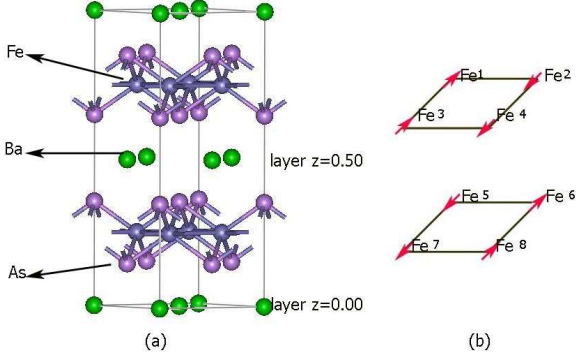


FIG. 1: (Color online) (a) The crystal structure of the $\sqrt{2} \times \sqrt{2} \times 1$ BaFe_2As_2 supercell. (b) The two Fe planes in the supercell. Red arrows show the AFM4 configuration.

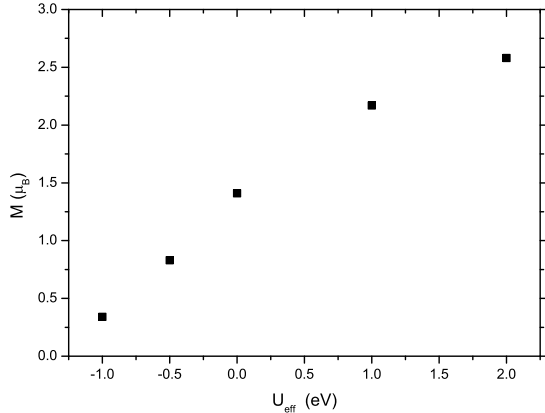


FIG. 2: The calculated magnetic moment of the AFM4 state of the $\sqrt{2} \times \sqrt{2} \times 1$ BaFe_2As_2 with different U_{eff} .

orbital intra-exchange energy (Hund's parameter)³³. Here we adopt a negative U_{eff} of -0.5 eV, and if not specially mentioned, all the discussions in the results are based on $U_{eff} = -0.5$ eV.

III. RESULTS AND DISCUSSIONS

First, we focus on the electronic properties of the mother compound BaFe_2As_2 . In order to describe the electronic structures with different magnetic orderings, the Fe atoms in two

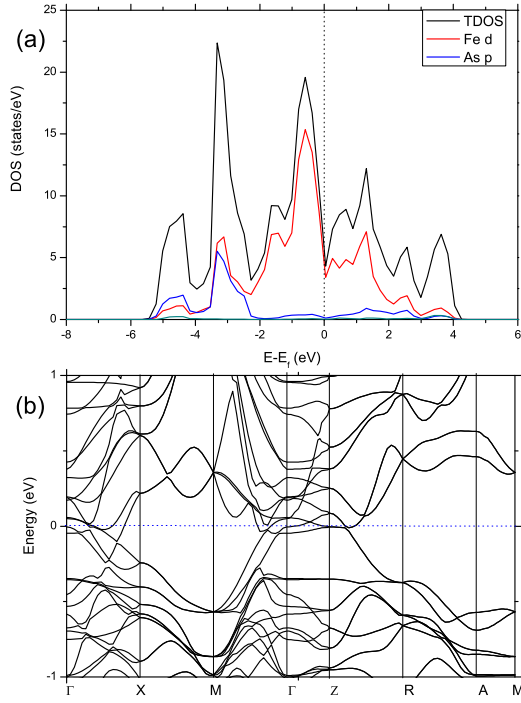


FIG. 3: (Color online) The total DOS and the projected DOS of the Fe d states and the As p states of the AFM4 state of the $\sqrt{2} \times \sqrt{2} \times 1$ BaFe₂As₂. Since the spin-up and spin-down states are degenerated for AFM states, we plot the spin-up channel only.

planes are numbered as in fig.1 (b). Except for the nonmagnetic(NM) and ferromagnetic (FM) states, the system have six possible AFM states: square-like in-plane AFM with Fe atoms directly above each other in the c-direction aligned parallelly, AFM1 $(-, -, +, +, -, -, +, +)$, and antiparallelly, AFM2 $(-, -, +, +, +, +, -, -)$; stripe-like in-plane AFM with Fe atoms directly above each other in the c-direction aligned parallelly AFM3 $(-, +, -, +, +, -, +, -)$, and antiparallelly AFM4 $(-, +, -, +, -, +, +, -, +)$; one plane with square-like AFM and the other with stripe-like AFM, AFM5 $(-, -, +, +, +, -, +, -)$; and in-plane FM with two planes aligned antiparallelly, AFM6 $(-, -, -, -, +, +, +, +)$. We initialize the systems with these NM, FM and six AFM orderings. After SCF calculations, the AFM1, AFM2, and AFM3 states converge to the NM state. The instabilities of NM state to other magnetic states, and the corresponding magnetic moment of Fe in these magnetic states are listed in Table I and II. We find very weak instabilities from NM to FM and AFM6, a stronger one to AFM5, and the strongest

TABLE I: The calculated magnetic instabilities of $\text{Ba}_{1-x}\text{K}_x\text{Fe}_2\text{As}_2$ ($x=0.00, 0.25, 0.50$ and 1.00). In the cases of same doping level, the lowest energy among the NM states is set to zero, energy with other magnetic configuration is the difference to it. ($E - E_{NM}$). The energy unit is meV.

	NM	FM	AFM1	AFM2	AFM3	AFM4	AFM5	AFM6
BaFe_2As_2	0.00	-0.89	—	—	—	-72.65	-37.04	-0.06
$\text{Ba}_{0.75}\text{K}_{0.25}\text{Fe}_2\text{As}_2$	case 1	0.02	—	—	—	-91.49	-45.42	—
	case 2	0.00	—	—	—	-95.40	-91.12	-45.26
$\text{Ba}_{0.50}\text{K}_{0.50}\text{Fe}_2\text{As}_2$	case 1	161.48	157.92	—	161.94	—	97.55	130.38
	case 2	161.20	157.47	—	164.89	—	96.22	129.94
	case 3	0.00	-18.32	-0.28	0.33	-88.92	-88.86	-44.01
$\text{Ba}_{0.25}\text{K}_{0.75}\text{Fe}_2\text{As}_2$	case 1	0.00	-42.20	-9.53	-14.82	—	-54.21	-36.20
	case 2	0.00	-42.21	-9.53	-14.84	-57.86	-54.26	-36.23
KFe_2As_2	0.00	-7.15	-30.30	—	—	1.97	-15.84	-39.20

instability to AFM4, which is the ground state. This ground state is consistent with the previous experimental result²⁴ and other calculations³⁴, where the ground state of BaFe_2As_2 was found to be stripe-like AFM with Fe atoms aligned antiparallelly to each other in c-direction. The magnetic moment we obtained for the ground state is about $0.83 \mu_B/\text{Fe}$, comparing with that in other calculations (about $2.67 \mu_B/\text{Fe}$), our result agrees much better with the experimental one ($0.87 \mu_B/\text{Fe}$).

We have tested the effects of different U_{eff} on the magnetic moments and total energies. As shown in fig. 2, the magnetic moment changes monotonously with U_{eff} , and a slight change of the U_{eff} will significantly alter the magnetic moment. Similar results have been found in ReFeAsO ,²⁸ a negative effective U thus may be a common feature of the FeAs layers.

The density of states (DOS) of the AFM4 state is shown in fig. 3a, similar to that in ReFeAsO , the contributions from Fe and As dominate the DOS near the fermi level, and the density of states at the fermi level (N_{E_f}) is 5.65. The band structure of AFM4 is illustrated in fig. 3b, the small dispersions along c axis (from Γ to Z and A to M) indicate the interactions between layers are small. There are three bands cross the fermi level, one electron band around Γ to X, and two hole bands around Γ to Z and M to Γ , which indicates

TABLE II: The calculated magnetic moments in μ_B per Fe atoms of $\text{Ba}_{1-x}\text{K}_x\text{Fe}_2\text{As}_2$ ($x=0.00, 0.25, 0.50$ and 1.00).

	FM	AFM1	AFM2	AFM3	AFM4	AFM5	AFM6
BaFe_2As_2	0.06	—	—	—	0.83	0.02, 0.85	0.03
$\text{Ba}_{0.75}\text{K}_{0.25}\text{Fe}_2\text{As}_2$	case 1	—	—	—	0.81	0.01, 0.81	—
	case 2	—	—	—	0.82	0.81	0.01, 0.81
$\text{Ba}_{0.50}\text{K}_{0.50}\text{Fe}_2\text{As}_2$	case 1	0.20	—	0.12	—	0.78	0.35, 0.76
	case 2	0.20	—	0.33, 0.35	—	0.78	0.14, 0.77
	case 3	0.25	0.13	0.51	0.83	0.84	0.39, 0.83
$\text{Ba}_{0.25}\text{K}_{0.75}\text{Fe}_2\text{As}_2$	case 1	0.31	0.57	0.63	—	0.78	0.80, 0.84
	case 2	0.31	0.57	0.63	0.80	0.79	0.79, 0.84
KFe_2As_2	0.44	1.10	—	—	0.61	0.58, 0.74, 1.04, 1.06	0.30

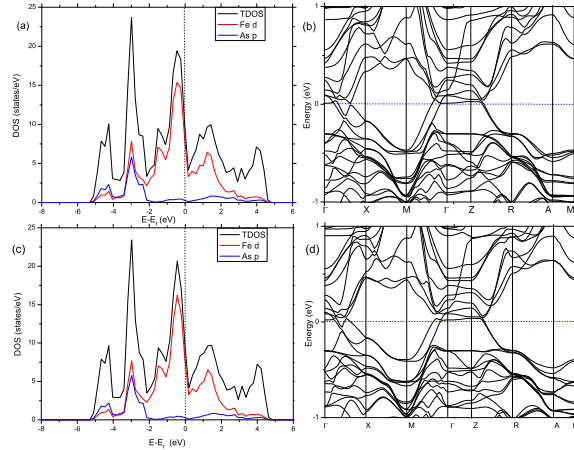


FIG. 4: (Color online) (a) DOS and (b) band structure of the AFM4 state of case 1, (c) DOS and (d) band structure of the AFM3 state of case 2 for $\text{Ba}_{0.75}\text{K}_{0.25}\text{Fe}_2\text{As}_2$.

the multi-band feature of the system.

Next, we turn to the doping effects on the electronic structure of the system. In the case of one K replace of Ba ($\text{Ba}_{0.75}\text{K}_{0.25}\text{Fe}_2\text{As}_2$), the K site has two choices, one is in the layer of $z=0.0$ (case1), and the other is in the layer of $z=0.5$ (case2), where z is the direct coordinate along the c axis of the supercell. The total energies of these two cases are very close, for NM

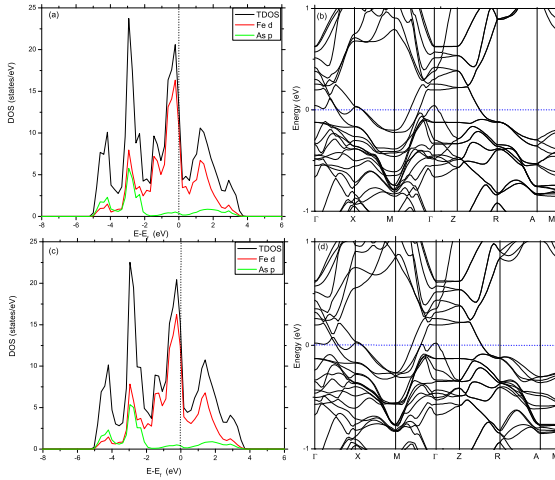


FIG. 5: (Color online)(a) DOS and (b) band structure of the AFM3 state, (c) DOS and (d) band structure of the AFM4 state for $\text{Ba}_{0.5}\text{K}_{0.5}\text{Fe}_2\text{As}_2$.

state, the total energy of case 1 is about 0.2 meV higher than that of case2. The results of magnetic instabilities and the magnetic moment on Fe of these two cases are listed in Table I and II. We find the AFM3 state disappears in case1, while in case2, it is the state has the lowest energy, and the magnetic moment on Fe is not significantly changed in the states with the in-plane stripe-like AFM.

The DOS and band structures of AFM4 of case1 and AFM3 of case2 are illustrated in fig. 4. Compared with the parent compound, the shape of the DOS does not alter significantly, but the states near the fermi level are shifted up, resulted in an increase of the N_{E_f} , which is 9.46 in AFM4 of case1, and 9.18 in AFM3 of case2. In the band structures, the changes of the states near the fermi level is much clearer, in both AFM4 of case1 and AFM3 of case2, only two hole bands across the fermi level, this is accord with the experimental results where hole pockets at Γ sites become larger after doping.²⁵

Then, we go to the case of $\text{Ba}_{0.5}\text{K}_{0.5}\text{Fe}_2\text{As}_2$. There are three possible ways of substitution for K, that is two in the layer $z=0.0$ (case 1), two in the layer $z=0.5$ (case 2) and one in each layer (case 3). The calculations show case 3 is the most favorable in the energy point of view, for NM state, the total energy of case 3 is about 0.19 eV lower than that of case 1 and case 2 per supercell. Thus, here we discuss the magnetic and electronic properties of case3 only. As shown in Table I and II, although AFM3 is the state with the lowest energy,

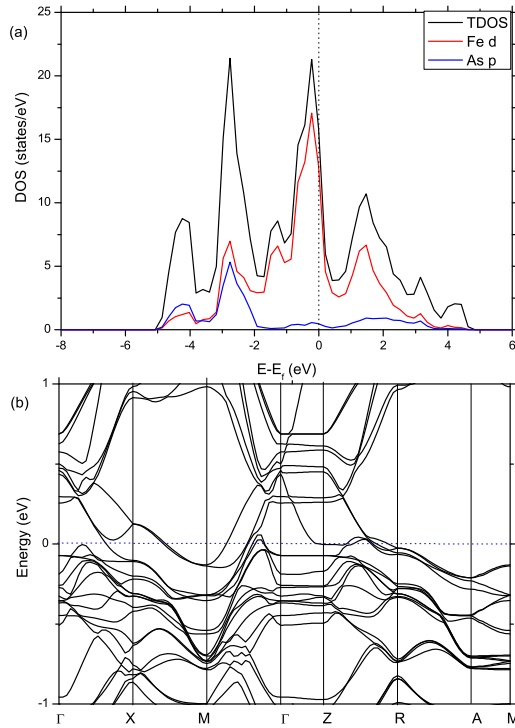


FIG. 6: (Color online) (a) DOS and (b) band structure of the AFM3 state of $\text{Ba}_{0.25}\text{K}_{0.75}\text{Fe}_2\text{As}_2$.

AFM4 is very close to it, and the magnetic moments on Fe of these two states are almost the same. So AFM3 and AFM4 may co-exist at this doping level, competing with each other. The DOS and band structure of AFM3 and AFM4 are given in fig. 5, though the shape of the DOS is similar to former cases, the states are further slightly shifted up with N_{E_f} of 12.84 for AFM3 and 13.13 for AFM4. In the band structure, there are 3 bands across the fermi level.

For $\text{Ba}_{0.25}\text{K}_{0.75}\text{Fe}_2\text{As}_2$, K atoms have two choices, one is two atoms in layer $z=0.0$, and the other one in layer $z=0.5$ (case 1), the other choice is two in layer $z=0.5$, and the other one in layer $z=0.0$ (case 2). In spin-unpolarized calculations, these two cases have almost the same total energy (case 1 lower about 3.65 meV than case 2), so these two structures may co-exist at this doping level. Although with very close energy, their magnetic structures are different. In Table I, we can see the AFM3 state is not exist in case1, while in case2, it has the lowest energy. And again, we find the magnetic moments on Fe of the states with the in-plane stripe-like AFM are almost the same. Besides, at this doping level, we find the

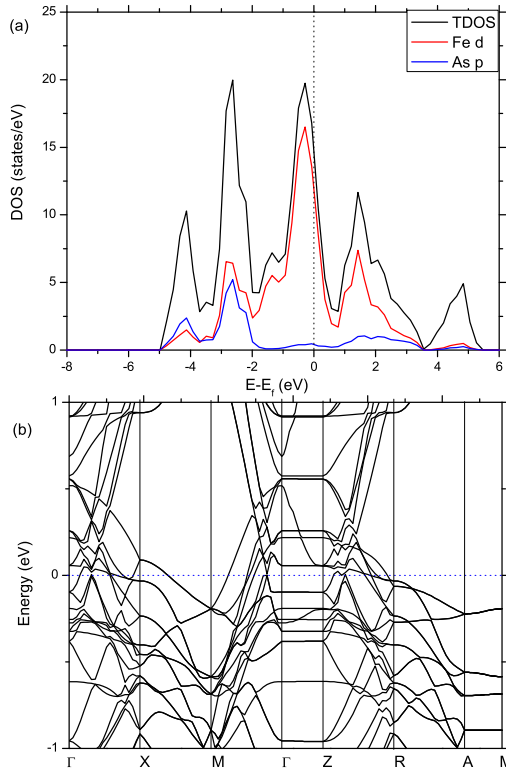


FIG. 7: (Color online) (a) DOS and (b) band structure of the AFM6 state for KFe_2As_2 .

instability from NM to FM is increased, close to that of NM to AFM4 or AFM3. So here, the system may have competing orders of FM, AFM3, and AFM4. In all states of case 1 and case 2, the AFM3 of case 2 has the lowest energy, the DOS and band structure of this state are plotted in fig. 6. The N_{E_f} in this case is increased to 15.24, and the bands near the fermi level are moved up, exhibiting 5 bands across the fermi level.

Lastly, although the 100% percent doping is hard to achieve in experiments, we still investigate this KFe_2As_2 case for consistency. The magnetic instabilities and magnetic moments on Fe atoms are given in Table I and II, we find the NM to AFM6 has the strongest instability here, with AFM1 the next. This is different with the above cases, where the states with in-plane stripe-like AFM is always the state with the lowest energy. The DOS and band structure are shown in fig. 7. Comparing with the DOS of $\text{Ba}_{0.25}\text{K}_{0.75}\text{Fe}_2\text{As}_2$, the N_{E_f} is slightly decreased to 14.70, and 5 bands cross the fermi level here.

From the results illustrated above, we find the magnetic properties of $\text{Ba}_{1-x}\text{K}_x\text{Fe}_2\text{As}_2$

is very sensitive to the doping geometry, and the magnetic moments highly depend on the ordering. These properties imply that the magnetism of these compounds is of itinerant character.³⁴ No matter the interlayer alignment of the states with in-plane stripe-like AFM, they have almost the same magnetic moments on Fe atoms. Doping does not change the nature that the DOS near the fermi level is dominated by the FeAs layer. It results in an increase of the N_{E_f} by shifting up the bands across the fermi level.

IV. CONCLUSION

In conclusion, we have performed first-principles calculation for $\text{Ba}_{1-x}\text{K}_x\text{Fe}_2\text{As}_2$ systems within the GGA+U method. Using a negative U_{eff} of -0.50 eV, we find the same SDW ground state with experiment for the parent compound, and the magnetic moment on Fe is very close to the experimental value (cal. $0.83 \mu_B$ v.s. exp. $0.87 \mu_B$). We predict the most favorable doping geometries from the energy point of view. Besides, we find that the magnetic instability is enhanced with $x=0.25$, and then start to decrease. Moreover, in our result, the magnetic structure is very sensitive to the geometry, and the magnetic moment on Fe highly depends on ordering, especially the in-plane ordering.

ACKNOWLEDGMENTS

This work was partially supported by the National Natural Science Foundation of China under Grant Nos. 20773112, 10574119, 50121202, and 20533030, by National Key Basic Research Program under Grant No. 2006CB922004, by the USTC-HP HPC project, and by the SCCAS and Shanghai Supercomputer Center.

* Corresponding author. E-mail: jlyang@ustc.edu.cn

¹ Y. Kamihara, T. Watanabe, M. Hirano, and H. Hosono, J. Am. Chem. Soc. **130**, 3296 (2008).

² X. H. Chen *et al.* Nature doi: 10.1038/nature07045 (2008); arXiv0803.3603 (2008)

³ G. F. Chen *et al.* arXiv:0803.4384 (2008)

⁴ Z. A. Ren *et al.* arXiv:0803.4283 (2008)

⁵ G. F. Chen *et al.* arXiv:0803.3790 (2008)

⁶ J. Yang *et al.* arXiv:0804.3727 (2008)

⁷ Z. A. Ren *et al.* arXiv:0803.2053 (2008)

⁸ Y. Kamihara *et al.* Nature **453**, 376 (2008)

⁹ D. J. Singh *et al.* Phys. Rev. Lett. **100**, 237003 (2008)

¹⁰ J. Dong *et al.* arXiv:0803.3246 (2008)

¹¹ C. de la Cruz *et al.* arXiv:0804.0795 (2008)

¹² H.-H. Wen, Gang Mu, Lei Fang, Huan Yang and Xiyu Zhu, Eur. Phys. Lett. **82**, 179009 (2008).

¹³ Z. A. Ren *et al.* arXiv:0804.2582 (2008)

¹⁴ M. Rotter, M. Tegel and D. Johrendt arXiv:0805.4630 (2008)

¹⁵ K. Sasmal *et al.* arXiv:0806.1301 (2008)

¹⁶ G. F. Chen *et al.* arXiv:0806.1209 (2008)

¹⁷ G. Wu *et al.* arXiv:0806.4279 (2008)

¹⁸ N. Ni *et al.* arXiv:0806.4328 (2008)

¹⁹ F. Ronning *et al.* arXiv:0806.4599 (2008)

²⁰ M. Rotter *et al.* arXiv:0805.4021 (2008)

²¹ L. X. Yang *et al.* arXiv:0806.2627 (2008)

²² H. Y. Liu *et al.* arXiv:0806.4806 (2008)

²³ F. J. Ma, Zhong-Yi Lu, and T. Xiang arXiv:0806.3526 (2008)

²⁴ Q. Huang *et al.* arXiv:0806.2776 (2008)

²⁵ C. Liu *et al.* arXiv:0806:3453 (2008)

²⁶ C. Krellner *et al.* arXiv:0806.1043 (2008)

²⁷ I. A. Nekrasov *et al.* arXiv:0806.2630 (2008)

²⁸ H. Nakamura *et al.* arXiv:0806.4804 (2008)

²⁹ H. Katayama-Yoshida *et al.* arXiv:0807.3770 (2008)

³⁰ G. Kresse and D. Joubert, Phys. Rev. B **59**, 1578 (1999); G. Kresse and J. Furthmuller, Phys. Rev. B **54**, 11169 (1996).

³¹ P. E. Blöchl, Phys. Rev. B **50**, 17953 (1994)

³² J. P. Perdew, K. Burke, and M. Ernzerhof, Phys. Rev. Lett. **77**, 3865 (1996)

³³ S. L. Dudarev, G. A. Botton, S. Y. Savrasov, C. J. Humphreys and A. P. Sutton, Phys. Rev. B **57**, 1505 (1998)

³⁴ D. J. Singh, arXiv:0807.2643 (2008)